

# Rate Meta-distribution in mmW D2D Networks with Beam Misalignment

Yibo Quan <sup>‡</sup> <sup>§</sup>, Marceau Coupechoux<sup>‡</sup> and Jean-Marc Kélib <sup>§</sup>

<sup>‡</sup> LTCI, Télécom Paris, Institut Polytechnique de Paris, 91120, Palaiseau, France

<sup>§</sup>Orange Labs, 92320, Châtillon, France

Email: {yibo.quan, marceau.coupechoux}@telecom-paris.fr, {jeanmarc.kelif}@orange.com

**Abstract**—This paper studies the coverage performance of device-to-device (D2D) communication under the millimeter wave (mmW) spectrum. The transmitter and receiver sides of users are equipped with directional antennas and adopt beamforming (BF). By considering a truncated Gaussian misalignment assumption, we derive computationally tractable expressions of the conditional rate coverage probability’s moments as a function of the number of antenna elements. The Beta approximation of the rate meta-distribution is obtained based on the first and the second moment. The numerical simulations confirm our analytical results. They show that the coverage performance can deteriorate significantly due to misalignment. Furthermore, an optimal number of antenna elements must be chosen to get the best coverage. In addition, there exists an optimal number of antennas which maximizes the number of users who satisfy the reliability constraints. This optimal value is a function of the reliability threshold.

**Index Terms**—Stochastic geometry, meta-distribution, beamforming, device-to-device, misalignment, URLLC.

## I. INTRODUCTION

5G mobile networks are envisioned to support ultra-reliable, and low latency communications (URLLC), which is targeted for a packet transmission with 99.999% reliability [1]. This stringent constraint calls for more innovations facing the rapid increase in data transmission demands. The device-to-device (D2D) communication concept, which allows direct communication without base stations, have been incorporated into 5G to reduce unnecessary connections or hops. Through this method, the traffic of the cellular network is mitigated by offloading the traffic to alternative side links [2]. However, employing D2D communication suffers from high interference and insufficient bandwidth. Exploiting the millimeter wave (mmW) bands seems to be a suitable solution for these problems [3], [4]. One of the critical drawbacks of mmW communication is that it faces vast propagation loss. The directional antenna arrays can be equipped to overcome the path loss, and beamforming (BF) can be adopted.

Because of its mathematical flexibility, stochastic geometry is widely used to evaluate the coverage, the throughput, and the energy efficiency of the mmW D2D networks [5]–[7]. The classical coverage probability refers to the average success probability among all the users. Under the context of URLLC, we are concerned not only by the network’s average performance but also by the distribution of the performance

metrics, e.g. to know what is the percentage of users satisfying the reliability requirements. The meta-distribution for D2D communication has thus been proposed to give a complete characterization of the spatial distribution of the communication reliability [7]. Initial results have been then extended in the literature. For example, the meta-distribution of the underlay D2D communication in a cellular network is studied in [8]. In [9] and [10], the meta-distribution for mmW D2D networks are derived, where only the D2D transmitters are equipped with multiple antennas.

In the existing works that study the meta-distribution of the mmW D2D network, the beam alignment is however supposed to be ideal. The maximum array gain is achieved by steering the main beam in the desired direction during the beam training period. However, in practice, a small misalignment error may provoke severe performance deterioration, which is confirmed by the existing works that study the coverage performance of cellular network [11]. It has also been shown in D2D networks [12], [13] in terms of coverage probability. Thus the beam alignment error cannot be neglected and there is no existing work studying the meta-distribution in conjunction with this type of error.

The contribution of this paper is summarized as follows:

- We provide a closed-form and computationally tractable formula for all the moments of the conditional rate coverage probability in D2D networks with perfect BF and antennas at both the transmitter and the receiver (see Theorem 1). We extend this result to the case of imperfect BF by considering a Gaussian misalignment model (see Theorem 2). The rate meta-distribution is then approximated using the Beta approximation.
- The simulations results show the accuracy of the analytical analysis and show that the Beta approximation provides a good estimate of the meta-distribution. They show that the coverage performance can deteriorate significantly due to misalignment.
- We highlight the existence of an optimal number of antennas that maximizes the (average) rate coverage probability which depends on the error magnitude. We also show that there is an optimal number of antennas maximizing the number of users satisfying a reliability requirement. This optimal number is dependent on the required reliability.

In the rest of this paper, we introduce the system model in Section II. Section III presents the analytical study of the rate meta-distribution. The numerical results are shown in Section IV. Section V concludes the paper.

## II. SYSTEM MODEL

We study the mmW D2D network by considering the classical bipolar network model [7]. The transmitter-receiver pairs are randomly located in a 2-dimensional space and perform point-to-point data transmissions. The D2D transmitters form a homogeneous Poisson point process (PPP)  $\Phi^T$  with intensity  $\lambda$ . Without loss of generality, we assume that each transmitter has a dedicated D2D receiver uniformly located on the circle around the transmitter, with a constant radius  $R$ . We denote the point process associated with the receivers by  $\Phi^R$ . A typical receiver is assumed to be at the origin and attempts to receive the data from the corresponding transmitter. According to the Slivnyak theorem, the statistical characteristics do not change for a PPP if we add a point in a particular position [14].

### A. Beamforming

To compensate for the visible mmW propagation loss, uniform linear array (ULA) is used at both transmitter and receiver ends. For each pair, the transmit and receive beams are required to be aligned toward each other. For the sake of mathematical tractability, we simplify the actual antenna pattern by the sectorized gain pattern based on the realistic pattern of ULA [15]. This model consists of a main beam and a side beam. The main beam gain is precisely the real maximum gain of ULA. The side beam gain is calculated without changing the average radiation intensity. Both transmitter and receiver antenna arrays have the same half power beamwidth (HPBW)  $\omega$ , which corresponds to the angular aperture of the main beam. For a ULA with  $n$  antenna elements, the HPBW can be expressed as a function of  $n$  as follows [15]:

$$\omega(n) = 2 \left( \frac{\pi}{2} - \arccos \frac{2.784}{n\pi} \right) \quad (1)$$

Let  $G_{max}^T$  and  $G_{min}^T$  represent the antenna gains of the main and side beams at transmitter's side. Respectively, we use  $G_{max}^R$  and  $G_{min}^R$  to denote the antenna gain of the main and side beams at receiver's side. Specifically, we have  $G_{max}^T = 2n$ ,  $G_{min}^T = \rho(n)$ ,  $G_{max}^R = 2n^2$  and  $G_{min}^R = n\rho(n)$  [15]. Here  $\rho$  is a function of  $n$  as shown in (2):

$$\rho(n) = \frac{\int_0^\pi \frac{2}{n} \left| \frac{\sin(\frac{1}{2}n\pi \cos \theta)}{\sin(\frac{1}{2}\pi \cos \theta)} \right|^2 d\theta - 2n\omega(n)}{\pi - \omega(n)} \quad (2)$$

To sum up, the array gain of a transmitter can be expressed as follows:

$$g_a^T(\theta, \theta_0^T) = \begin{cases} G_{max}^T, & 0 \leq |\theta - \theta_0^T| \leq \omega/2 \\ G_{min}^T, & \omega/2 \leq |\theta - \theta_0^T| \leq \pi/2 \\ 0, & \text{otherwise} \end{cases} \quad (3)$$

where  $\theta$  is the angle of departure (AoD) of the plane wave with respect to a the linear array's axis. We denote  $\theta_0^T$  as the

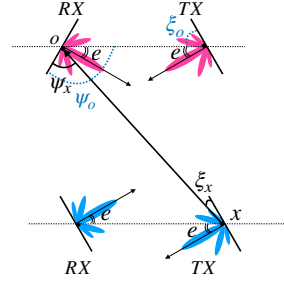


Fig. 1. Two D2D transmitter-receiver pairs (blue and rose) with misalignment.

boresight direction of the transmitter array (main lobe direction), which is decided by the beamformer [15]. Respectively, the array gain of a receiver  $g_a^R(\theta, \theta_0^R)$  has a main lobe of gain  $G_{max}^R$  within the same HPBW around its boresight direction  $\theta_0^R$ , and a sidelobe of gain  $G_{min}^R$ .

### B. Misalignment Model

Consider a typical receiver device at origin  $O$ . Then  $\psi_o$  is the angle of arrival (AoA) of the plane wave from its corresponding transmitter regarding the receiver antenna array's axis. Moreover,  $\xi_o$  is the AoD to the transmitter array's axis. We choose  $\theta_0^T = \theta_0^R = \pi/2$  to ensure that the antenna arrays are broadside antennas (boresight direction is perpendicular to the axis). Ideally, the transmitter and receiver should be face-to-face to align their main lobes of beams to each other. That is to say  $\psi_o = \xi_o = \pi/2$ . Nevertheless, the alignment is often not perfect in reality, so there is an alignment error  $e$  as shown in Fig. 1. Thus  $\psi_o$  and  $\xi_o$  can be modelled as random variables whose means are  $\theta_0^R$  and  $\theta_0^T$ . According to the central limit theorem, the truncated Gaussian distribution is a properly estimation of the alignment errors induced by multiple independent sources. We assume that the errors have a span from  $-\pi$  to  $\pi$ . The probability density function (PDF) of  $\xi_o$  or  $\psi_o$  can thus be expressed by using the truncated Gaussian distribution [16]:

$$f_\xi(x) = \frac{1}{\sqrt{2\pi}\sigma} \frac{\exp(-\frac{1}{2}(\frac{x-\theta_0^T}{\sigma})^2)}{\text{erf}(\frac{\pi}{\sqrt{2}\sigma})}, x \in [\theta_0^T - \pi, \theta_0^T + \pi] \quad (4)$$

### C. Channel Model

For a typical active receiver located at the origin  $O$  and its corresponding transmitter at  $x_o$ , the total antenna gain of this link is:

$$G_o(\xi_o, \psi_o) = g_a^R(\psi_o, \theta_0^R) g_a^T(\xi_o, \theta_0^T) \quad (5)$$

Consider a link between a receiver located at origin  $O$  and an interfering transmitter located at  $x$ . As shown in Fig. 1,  $\psi_x$  is the AoA with respect to receiver's array axis, and  $\xi_x$  is the AoD with respect to transmitter's array axis. Then the antenna gain of this link can be expressed as follows:

$$G_x(\xi_x, \psi_x) = g_a^R(\psi_x, \theta_0^R) g_a^T(\xi_x, \theta_0^T) \quad (6)$$

We are interested in the Shannon rate  $\mathcal{R}$ :

$$\mathcal{R} = W \log_2 \left( 1 + \frac{Ph_{x_o} G_o(\xi_o, \psi_o) \ell(R)}{\sum_{x \in \Phi \setminus x_o} Ph_x G_x(\xi_x, \psi_x) \ell(|x|) + \mathcal{N}_0 W} \right) \quad (7)$$

where  $\ell(\cdot)$  is the path gain function:  $\ell(x) = x^{-\beta}$ ,  $\beta \in \mathbb{N}^+$  and  $\beta > 2$ . The small-scale fading coefficient associated with the link from the transmitter at  $x$  to the receiver at origin is denoted by  $h_x$ , which has an exponential distribution with unit mean (Rayleigh fading). Moreover, all users transmit with the same power  $P$ . The noise power is  $\mathcal{N}_0 W$ , where  $\mathcal{N}_0$  and  $W$  are the noise power spectral density and the bandwidth, respectively.

### III. META DISTRIBUTION

The meta-distribution defined in [7] describes the spatial distribution of the devices' communications' reliability. Similar to the definition in [6], we define the rate meta-distribution as a two-parameter distribution function as follows:

$$\bar{F}_{P_s(\eta)}(\epsilon) \triangleq \mathbb{P}^l(P_s(\eta) > \epsilon), \quad \epsilon \in [0, 1], \theta \in \mathbb{R}^+. \quad (8)$$

where  $P_s(\eta)$  is the conditional rate coverage probability or the conditional success probability:

$$P_s(\eta) \triangleq \mathbb{P}(\mathcal{R} > \eta | \Phi^T, \Phi^R) \quad (9)$$

The classical coverage probability is its mean. The notation  $\mathbb{P}^l$  denotes the Palm measure of  $\{\Phi^T, \Phi^R\}$ , given that there is an active receiver at the prescribed location. During a long period, users may experience different communication conditions. Thus the conditional rate coverage probability describes the temporal success probability of a certain user. We call the threshold  $\epsilon$  as the reliability threshold of the network. It is assumed that the communication is reliable if the probability of the user getting a rate higher than  $\eta$  is larger than  $\epsilon$ . Then the rate meta-distribution  $\bar{F}_{P_s(\eta)}(\epsilon)$  is designed to characterize the spatial distribution of reliability.

#### A. Moments of the conditional rate coverage probability

**Theorem 1.** Consider a D2D network with the BF model introduced in Section II. If the beam alignment is perfect, the  $b$ -th moment of the conditional rate coverage probability  $M_b(\eta)$  has the following expression:

$$M_b(\eta) = \exp \left( -b\eta' \frac{\mathcal{N}_0 W}{PG_o(\xi_o, \psi_o)} \right) \exp(-\lambda Q_b(\eta)) \quad (10)$$

where  $\eta' = \frac{2^{\frac{\eta}{W}} - 1}{\ell(R)}$ , and  $Q_b(\eta)$  is a function of  $b$  and  $\eta$ :

$$\begin{aligned} Q_b(\eta) = & \lim_{T \rightarrow \infty} \frac{T^\delta \delta \pi}{4} \sum_{n=1}^{\infty} \binom{b}{n} (-1)^{n+1} B(\delta, 1) \\ & \times \left( p^2 {}_2F_1(n, \delta, \delta + 1, \frac{-G_o(\xi_o, \psi_o) T}{G_1 \eta'}) \right. \\ & + 2p(1-p) {}_2F_1(n, \delta, \delta + 1, \frac{-G_o(\xi_o, \psi_o) T}{G_2 \eta'}) \\ & \left. + (1-p)^2 {}_2F_1(n, \delta, \delta + 1, \frac{-G_o(\xi_o, \psi_o) T}{G_3 \eta'}) \right) \quad (11) \end{aligned}$$

where  $p = \omega/\pi$ ,  $\delta = 2/\beta$ ,  $G_1 = 4n^3$ ,  $G_2 = 2n^2\rho$  and  $G_3 = n\rho^2$ . Function  $B(\cdot, \cdot)$  is the Beta function and  ${}_2F_1(\cdot)$  is the hyper-geometric function.

*Proof.* The proof is a special case of the proof of theorem 2.  $\square$

#### B. Impact of misalignment

We define the matching probability as  $p_{ma}$ , which refers to the case where  $\xi_o$  (respectively  $\psi_o$ ) is within the HPBW around  $\theta_0^T$  (respectively  $\theta_0^R$ ):

$$p_{ma} = \int_{\theta_0^T - \frac{\pi}{2}}^{\theta_0^T + \frac{\pi}{2}} f_{\xi_o} d\xi_o \quad (12)$$

The effective probability  $p_{ef}$  specifies the probability that  $\xi_o$  or  $\psi_o$  is within  $[0, \pi]$ :

$$p_{ef} = \int_{\theta_0^T - \frac{\pi}{2}}^{\theta_0^T + \frac{\pi}{2}} f_{\xi_o} d\xi_o \quad (13)$$

With these notations, we have the following result:

**Theorem 2.** With beam misalignment, the  $b$ -th moment of the conditional rate coverage probability has the following expression:

$$\begin{aligned} M_b = & p_{ma}^2 \exp \left( -b\eta' \frac{\mathcal{N}_0 W}{PG_1} \right) \exp(-\lambda Q_b(G_1, \eta)) \\ & + 2p_{ma}(p_{ef} - p_{ma}) \exp \left( -b\eta' \frac{\mathcal{N}_0 W}{PG_2} \right) \exp(-\lambda Q_b(G_2, \eta)) \\ & + (p_{ef} - p_{ma})^2 \exp \left( -b\eta' \frac{\mathcal{N}_0 W}{PG_3} \right) \exp(-\lambda Q_b(G_3, \eta)) \quad (14) \end{aligned}$$

where  $Q_b(G_o, \eta)$  has the same expression as the right hand side of the formula (11).

*Proof.* See Appendix A.  $\square$

#### C. Beta approximation

The numerical computation of the exact rate meta-distribution by using Gil-Pélaez theorem [7] is often difficult. An alternative solution is to approximate it with a Beta-distribution [7] by matching the first and the second moment as follows:

$$\bar{F}_{P_s(\eta)}(\epsilon) = 1 - I_\epsilon \left( \frac{M_1 M_2 - M_1^2}{M_1^2 - M_2}, \frac{(1 - M_1)(M_2 - M_1)}{M_1^2 - M_2} \right) \quad (15)$$

where  $I_\epsilon(\cdot)$  is the regularized incomplete beta function [9].

### IV. NUMERICAL SIMULATION

At the beginning of the simulation, a specific configuration of the network is decided by randomly choosing the locations of the devices, where the location for each transmitter is uniformly chosen in the plane, and the position of its corresponding receiver is uniformly chosen on a circle of radius  $R$  around it. Assuming such a fixed spatial configuration, we draw the value of the random variable  $h_x$  for every link. The Shannon rate is calculated for each receiver, and we count the

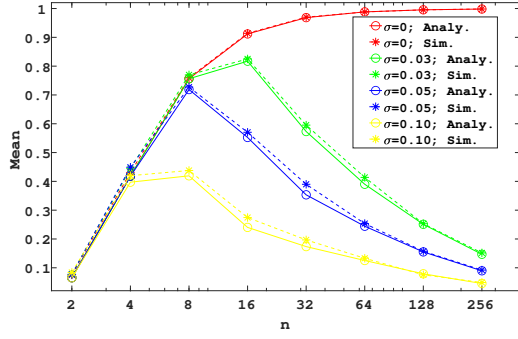


Fig. 2. Mean of  $P_s(\eta)$  as a function of  $n$  with misalignment.

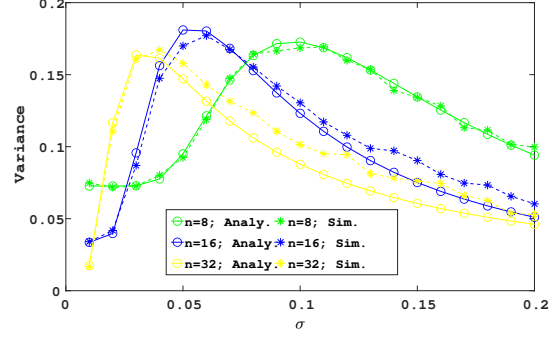


Fig. 4. Variance of  $P_s(\eta)$  as a function of  $\sigma$  with misalignment.

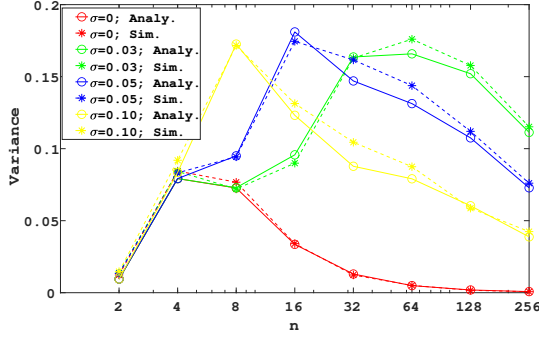


Fig. 3. Variance of  $P_s(\eta)$  as a function of  $n$  with misalignment.

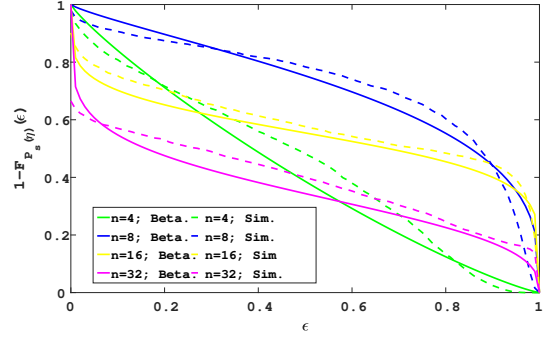


Fig. 5. Meta distribution with misalignment.

number of success transmissions for each pair for a given rate threshold  $\eta$ . This process is repeated for sufficient number of iterations in order to get the rate meta-distribution. Network parameters are as follows:  $W = 1$  MHz,  $\beta = 3.5$ ,  $R = 30$  m,  $\lambda = 0.01 \text{ m}^{-2}$  and  $\eta = 1$  Mbps. The standard deviation in Fig. 5 is  $\sigma = 0.05$ .

Fig. 2 shows the mean of  $P_s(\eta)$  as a function of  $n$ , in presence of Gaussian misalignment. The solid curves show the analytical results derived from (14). The dotted curves are from the simulations results. The two sets of curves are very close. When there is no misalignment, the average of  $P_s(\eta)$  is increasing with the number of antennas. This can be explained by the thinner beams which increase the useful received signal power while reducing interference. When there are misalignment errors, the coverage probability is decreasing with the error amplitude. Moreover, the average coverage probability is characterized by an optimal number of antennas. Thinner beams are indeed more prone to misalignment errors leading to a loss of coverage when the error is large. The optimal number of antennas is a decreasing function of the error magnitude due to this effect.

Figs. 3 and 4 show the variance of  $P_s$  as a function of the number of antennas and of the error magnitude, respectively. The difference between the simulation and the analytical results is again relatively small. When  $\sigma$  is small, the variance is small because the coverage is good enough in most cases. On the contrary, most users cannot be covered when the error

is strong, so the variance is also small. There is however an intermediate zone where sometimes users are connected, sometimes not, and the variance is relatively strong. This explains the bell shapes of the curves. The value of  $\sigma$ , which gives the maximum variance, gets smaller when the number of antennas increases. This is because the beam is thinner and we thus enter the intermediate interval with lower errors.

For a given value of the reliability threshold  $\epsilon$ , we can interpret the meta distribution as follows: There is a proportion  $1 - F_{P_s(\eta)}(\epsilon)$  of users who meet the reliability requirement. The function  $\epsilon \mapsto 1 - F_{P_s(\eta)}(\epsilon)$  is precisely the complementary cumulative distribution function (CCDF) of  $P_s(\eta)$ , which is shown in Fig. 5. The dotted curves are obtained by Monte Carlo simulations, and the solid curves are the Beta approximation results.

First, note that the Beta approximation is a sufficiently good approximation to analyze main performance trends. Curves are decreasing because, if the reliability threshold increases, there are less and less users meeting the requirement (see (8)). For a fixed threshold  $\epsilon$ , if a curve is above another, it means that more users are meeting the reliability requirement; as a consequence, the higher is the curve, the more reliable is the network. Having this in mind, we see for example that  $n = 8$  maximizes reliability for  $\epsilon$  between 0 and 0.9 approximately, but then  $n = 16$  is the best option. There is thus an optimal number of antennas which depends on the reliability threshold.

This also illustrates the fact that the best coverage does

not always imply the best reliability. When  $\sigma = 0.05$ , Fig. 2 shows that 4 antennas leads to a better average rate coverage than 32 antennas. However, according to Fig. 5, we find that 32 antennas can cover more users if the reliability threshold is high enough. These two metrics can be combined together to evaluate the network performance comprehensively.

## V. CONCLUSION

In this paper, we study the rate meta-distribution in a mmW D2D network with beamforming. Transmitters and receivers are both equipped with multiple antennas. The impacts of beam misalignment under a truncated Gaussian alignment error model are investigated. Our analytical and numerical results show a strong impact of beam misalignment which cannot be neglected in the analysis of coverage and when requiring a certain reliability. We show that there exists an optimal number of antennas that maximizes the (average) rate coverage probability. This optimal number depends on the error magnitude and the rate threshold. We also show that there is an optimal number of antennas which maximizes the number of users satisfying a reliability requirement. Moreover, this optimal number is dependent on the required reliability.

## APPENDIX A

Consider only the randomness of  $h_{x_o}$ . The conditional probability  $\mathbb{P}(\mathcal{R} > \eta | \Phi^T, \Phi^R, h_x)$  is a constant for given configuration  $(\Phi^T, \Phi^R)$  and given value of  $h_x$ , for all  $x \in \Phi^T \setminus x_o$ . According to the definition of rate in (7), it follows:

$$\begin{aligned} & \mathbb{P}(\mathcal{R} > \eta | \Phi^T, \Phi^R, h_x) \\ &= \mathbb{P}\left(h_{x_o} > \eta' \frac{\sum_{x \in \Phi^T \setminus x_o} P h_x G_x(\xi_x, \psi_x) \ell(|x|) + \mathcal{N}_0 W}{G_o(\xi_o, \psi_o) P} \right. \\ & \quad \left. | \Phi^T, \Phi^R, h_x\right) \quad (16) \\ &= \exp\left(-\eta' \frac{\sum_{x \in \Phi^T \setminus x_o} P h_x G_x(\xi_x, \psi_x) \ell(|x|) + \mathcal{N}_0 W}{G_o(\xi_o, \psi_o) P}\right) \quad (17) \end{aligned}$$

where  $\eta' = \frac{2^{\frac{\eta}{R}} - 1}{\ell(R)}$  and (18) comes from the fact that  $h_{x_o}$  is exponentially distributed with unit mean. The conditional rate coverage probability  $P_s(\eta)$  can be written as follows:

$$\begin{aligned} P_s(\eta) &= \mathbb{E}_{h_x} [\mathbb{P}(\mathcal{R} > \eta | \Phi^T, \Phi^R, h_x)] \\ &= \mathbb{E}_{h_x} \left[ \mathcal{L}_N \prod_{x \in \Phi^T \setminus x_o} \exp\left(-\eta' \frac{G_x(\xi_x, \psi_x)}{G_o(\xi_o, \psi_o)} h_x \ell(|x|)\right) \right] \quad (18) \\ &= \mathcal{L}_N \prod_{x \in \Phi^T \setminus x_o} \frac{G_o(\xi_o, \psi_o)}{\eta' G_x(\xi_x, \psi_x) \ell(|x|) + G_o(\xi_o, \psi_o)} \quad (19) \end{aligned}$$

where  $\mathcal{L}_N = \exp\left(-\eta' \frac{\mathcal{N}_0 W}{P G_o(\xi_o, \psi_o)}\right)$ . We get (19) because the channels  $h_x$ ,  $x \in \Phi^T$  are supposed to be i.i.d.. Each follows

an exponential distribution with unit mean. The  $b$ 's moment of  $P_s(\eta)$  is the expectation of  $P_s(\eta)^b$  w.r.t.  $\Phi^T$  and  $\Phi^R$ :

$$\begin{aligned} M_b(\eta) &= \mathbb{E}_{\Phi^T} [\mathbb{E}_{\Phi^R} [(\mathcal{L}_N \times \\ & \quad \prod_{x \in \Phi^T \setminus x_o} \frac{G_o(\xi_o, \psi_o)}{\eta' G_x(\xi_x, \psi_x) \ell(|x|) + G_o(\xi_o, \psi_o)})^b]] \quad (20) \\ &= \mathcal{L}_N \times \\ & \quad \mathbb{E}_{\Phi^T} \left[ \prod_{x \in \Phi^T \setminus x_o} \mathbb{E}_{\xi_x} \left[ \left( \frac{G_o(\xi_o, \psi_o)}{\eta' G_x(\xi_x, \psi_x) \ell(|x|) + G_o(\xi_o, \psi_o)} \right)^b \right] \right] \quad (21) \\ &= \mathcal{L}_N \exp(-\lambda Q_b(\eta)) \quad (22) \end{aligned}$$

where

$$\begin{aligned} Q_b(\eta) &= \\ & \int_{\mathbb{R}^2} \left( 1 - \mathbb{E}_{\xi_x} \left[ \left( \frac{G_o(\xi_o, \psi_o)}{\eta' G_x(\xi_x, \psi_x) \ell(|x|) + G_o(\xi_o, \psi_o)} \right)^b \right] \right) dx \quad (23) \end{aligned}$$

We get (21) because  $\psi_x$  and  $|x|$  are deterministic values once  $\Phi^R$  is fixed. The relative directions  $\xi_o$  and  $\psi_o$  within the typical pair are independent on  $\Phi^T$  and  $\Phi^R$ . The process  $\Phi^R$  is a conditional random measure that depends both on  $\Phi^T$  and  $\{\xi_x\}$ ,  $x \in \Phi^T$ , where  $\xi_x$  for different  $x \in \Phi^T$  are independent. So the expectation with respect to  $\Phi^R$  in (20) can be replaced by the expectation with respect to  $\xi_x$  in (21). The equation (22) follows from the probability generation functional (PGFL) of a Poisson point process [17]. We then transform the integral part  $Q_b$  into polar form. Since  $G_x(\xi_x, \psi_x) = 0$  when  $-\pi < \psi_x < 0$ , we get:

$$\begin{aligned} Q_b(\eta) &= \int_0^\infty \int_0^\pi \left( 1 - \right. \\ & \quad \left. \mathbb{E}_{\xi_x} \left[ \left( \frac{G_o(\xi_o, \psi_o)}{\eta' G_x(\xi_x, \psi_x) \ell(v) + G_o(\xi_o, \psi_o)} \right)^b \right] \right) d\psi_x v dv \quad (24) \end{aligned}$$

Remind that  $\xi_x$  is uniformly distributed in  $[0, 2\pi]$ . Given that  $G_x(\xi_x, \psi_x) = 0$  when  $\pi < \xi_x < 2\pi$ , the integral  $Q_b$  has the following form:

$$\begin{aligned} Q_b(\eta) &= \frac{1}{2\pi} \int_0^\infty \int_0^\pi \int_0^\pi \left( 1 - \right. \\ & \quad \left. \left( 1 - \frac{\eta' G_x(\xi_x, \psi_x) \ell(v)}{\eta' G_x(\xi_x, \psi_x) \ell(v) + G_o(\xi_o, \psi_o)} \right)^b \right) v d\xi_x d\psi_x dv \quad (25) \\ &= \frac{1}{2\pi} \int_0^\infty \int_0^\pi \int_0^\pi \left[ 1 - \right. \\ & \quad \left. \sum_{k=0}^{\infty} \binom{b}{k} \left( -\frac{\eta' G_x(\xi_x, \psi_x) \ell(v)}{\eta' G_x(\xi_x, \psi_x) \ell(v) + G_o(\xi_o, \psi_o)} \right)^k \right] v d\xi_x d\psi_x dv \quad (26) \end{aligned}$$

where (26) comes from the binomial series.

$$Q_b(\eta) = \frac{1}{2\pi} \sum_{n=1}^{\infty} \binom{b}{n} (-1)^{n+1} \times \int_0^{\infty} \int_0^{\pi} \int_0^{\pi} \left( \frac{\eta' G_x(\xi_x, \psi_x) \ell(v)}{\eta' G_x(\xi_x, \psi_x) \ell(v) + G_o(\xi_o, \psi_o)} \right)^n v d\xi_x d\psi_x dv \quad (27)$$

Let  $u = v^\beta$  and  $\delta = 2/\beta$ . For  $b \in \mathbb{C}$  we have :

$$Q_b(\eta) = \lim_{T \rightarrow \infty} \frac{\delta}{4\pi} \sum_{n=1}^{\infty} \binom{b}{n} (-1)^{n+1} \times \int_0^T \int_0^{\pi} \int_0^{\pi} \left( \frac{\eta' G_x(\xi_x, \psi_x)}{\eta' G_x(\xi_x, \psi_x) + G_o(\xi_o, \psi_o) u} \right)^n u^{\delta-1} d\xi_x d\psi_x du \quad (28)$$

By replacing  $u$  with  $r = u/T$ , we get:

$$Q_b(\eta) = \lim_{T \rightarrow \infty} \frac{T^\delta \delta}{4\pi} \sum_{n=1}^{\infty} \binom{b}{n} (-1)^{n+1} \times \int_0^1 \int_0^{\pi} \int_0^{\pi} \left( \frac{\eta' G_x(\xi_x, \psi_x)}{\eta' G_x(\xi_x, \psi_x) + G_o(\xi_o, \psi_o) T r} \right)^n r^{\delta-1} d\xi_x d\psi_x dr \quad (29)$$

By adapting the definitions of  $g_a^R(\psi_x, \theta_0^R)$  and  $g_a^T(\xi_x, \theta_0^T)$ , the gain  $G_x$  has three non-negative values  $G_1$ ,  $G_2$  and  $G_3$  with probability  $p^2$ ,  $2p(1-p)$  and  $(1-p)^2$ . The notation  $Q_b$  can be then written as follows:

$$Q_b = \lim_{T \rightarrow \infty} \frac{T^\delta \delta \pi}{4} \sum_{n=1}^{\infty} \binom{b}{n} (-1)^{n+1} \int_0^1 \left( \frac{p^2}{\left(1 + \frac{G_o(\xi_o, \psi_o) r T}{G_1}\right)^n} + \frac{2(1-p)p}{\left(1 + \frac{G_o(\xi_o, \psi_o) r T}{G_2}\right)^n} + \frac{(1-p)^2}{\left(1 + \frac{G_o(\xi_o, \psi_o) r T}{G_3}\right)^n} \right) r^{\delta-1} dr \quad (30)$$

The final expression in (11) is derived by replacing the integral parts into hypergeometric functions.

When there is misalignment, the additional misalignment of  $\xi_o$  or  $\psi_o$  doesn't impact the distributions of  $\xi_x$  nor  $\psi_x$ . Because  $\xi_x$  and  $\psi_x$  are all uniformly distributed with respect to independent transmitters at  $x$ . So the only factor that is impacted in (10) and (11) is  $G_o$ . We define  $Q_b(G_o, \eta)$  as a function of  $G_o$ . It has the same expression as the right hand side of (11). According to the definition of  $G_o$  in (5) and the definition of  $g_a^R(\psi_o, \theta_0^R)$ ,  $g_a^T(\xi_o, \theta_0^T)$ , it is straightforward to give the probability mass function (PMF) of  $G_o$  as follows:

$$G_o = \begin{cases} G_1 & p_{ma}^2 \\ G_2 & 2p_{ma}(p_{ef} - p_{ma}) \\ G_3 & (p_{ef} - p_{ma})^2 \\ 0 & else \end{cases} \quad (31)$$

Therefore when there is misalignment, the  $b$ 's moment of  $P_s(\eta)$  is the expectation of  $P_s(\eta)^b$  with respect to  $\Phi^T$ ,  $\Phi^R$  and also  $G_o$ . The expression (14) is obtained by calculating the expectation of formula (10) with respect to  $G_o$ .

## REFERENCES

- [1] 3GPP, "3GPP Release 16," , Technical Specification (TS), 2018. [Online]. Available: <https://www.3gpp.org/release-16>
- [2] M. S. Gismalla, A. I. Azmi, M. R. Salim, M. F. Abdullah, F. Iqbal, W. A. Mabrouk, M. Othman, A. Y. Ashyap, and A. S. M. Supa'at, "Survey on Device to Device (D2D) communication for 5gb/6g networks: Concept, applications, challenges, and future directions," *IEEE Access*, 2022.
- [3] K. Venugopal, M. C. Valenti, and R. W. Heath, "Device-to-Device millimeter wave communications: Interference, coverage, rate, and finite topologies," *IEEE Transactions on Wireless Communications*, vol. 15, no. 9, pp. 6175–6188, 2016.
- [4] N. Bahadori, N. Namvar, B. Kelley, and A. Homaifar, "Device-to-Device communications in the millimeter wave band: A novel distributed mechanism," in *2018 Wireless Telecommunications Symposium (WTS)*. IEEE, 2018, pp. 1–6.
- [5] W. Yi, Y. Liu, and A. Nallanathan, "Modeling and analysis of D2D millimeter-wave networks with poisson cluster processes," *IEEE Transactions on Communications*, vol. 65, no. 12, pp. 5574–5588, 2017.
- [6] N. Deng and M. Haenggi, "The energy and rate meta distributions in wirelessly powered D2D networks," *IEEE Journal on Selected Areas in Communications*, vol. 37, no. 2, pp. 269–282, 2018.
- [7] M. Haenggi, "The meta distribution of the SIR in poisson bipolar and cellular networks," *IEEE Transactions on Wireless Communications*, vol. 15, no. 4, pp. 2577–2589, 2015.
- [8] M. Salehi, A. Mohammadi, and M. Haenggi, "Analysis of D2D underlaid cellular networks: SIR meta distribution and mean local delay," *IEEE Transactions on Communications*, vol. 65, no. 7, pp. 2904–2916, 2017.
- [9] N. Deng and M. Haenggi, "A fine-grained analysis of millimeter-wave Device-to-Device networks," *IEEE Transactions on Communications*, vol. 65, no. 11, pp. 4940–4954, 2017.
- [10] R. Wang, N. Deng, and H. Wei, "Towards a deep analysis of millimeter wave D2D underlaid cellular networks," *IEEE Transactions on Communications*, vol. 69, no. 10, pp. 6545–6560, 2021.
- [11] M. Cheng, J.-B. Wang, Y. Wu, X.-G. Xia, K.-K. Wong, and M. Lin, "Coverage analysis for millimeter wave cellular networks with imperfect beam alignment," *IEEE Transactions on Vehicular Technology*, vol. 67, no. 9, pp. 8302–8314, 2018.
- [12] J. Wildman, P. H. J. Nardelli, M. Latva-aho, and S. Weber, "On the joint impact of beamwidth and orientation error on throughput in directional wireless poisson networks," *IEEE Transactions on Wireless Communications*, vol. 13, no. 12, pp. 7072–7085, 2014.
- [13] N. Bahadori, N. Namvar, B. Kelley, and A. Homaifar, "Device-to-Device communications in millimeter wave band: Impact of beam alignment error," in *2019 Wireless Telecommunications Symposium (WTS)*. IEEE, 2019, pp. 1–6.
- [14] M. Haenggi, *Stochastic geometry for wireless networks*. Cambridge University Press, 2012.
- [15] Y. Quan, J.-M. Kelif, and M. Coupechoux, "Spatio-temporal wireless D2D network with beamforming," *IEEE International Conference on Communications (ICC)*, June 2021.
- [16] N. L. Johnson, S. Kotz, and N. Balakrishnan, *Continuous Univariate Distributions, Volume 1, 2nd Edition*. John Wiley and Sons, 1994.
- [17] F. Baccelli, B. Błaszczyszyn, and M. Karray, "Random measures, point processes, and stochastic geometry," 2020.